ISSN: 1410-8917
Jurnal Kimia Sains & Aplikasi
e-ISSN: 2597-9914

Jurnal Kimia Sains dan Aplikasi 25 (7) (2022): 235–244

Jurnal Kimia Sains dan Aplikasi
Journal of Scientific and Applied Chemistry

Journal homepage: http://ejournal.undip.ac.id/index.php/ksa

Preparation of $CoFe_2O_4/SiO_2/Ag$ Magnetic Composite as Photocatalyst for Congo Red Dye and Antibacterial Potential

Salni [a], Muhammad Said [b], Eliza [b], Anggun Dita Dyah Gayatri [b], Poedji Loekitowati Hariani [b,*]

[a] Department of Biology, Faculty of Mathematics and Natural Sciences, Universitas Sriwijaya, Ogan Ilir, Indonesia
[b] Department of Chemistry, Faculty of Mathematics and Natural Sciences, Universitas Sriwijaya, Ogan Ilir, Indonesia

*Corresponding author: puji_lukitowati@mipa.unsri.ac.id

https://doi.org/10.14710/jksa.25.7.235-244

Article Info

Article history:

Received: 12th June 2022
Revised: 20th July 2022
Accepted: 27th July 2022
Online: 31st August 2022

Keywords:
$CoFe_2O_4/SiO_2/Ag$; magnetic; photocatalyst; Congo red; antibacterial

Abstract

This research reports the synthesized $CoFe_2O_4/SiO_2/Ag$ magnetic composite used as a photocatalyst to degrade Congo red dye and antibacterial agent against *Staphylococcus aureus* (*S. aureus*) and *Escherichia coli* (*E. coli*). The catalysts were characterized using XRD, SEM-EDS, VSM, UV-DRS, and pH_{pzc}. The effects of photocatalyst dose (0.25, 0.5, 0.75, and 1.0 g/L), dye concentration (10, 20, 30, and 40 mg/L), and irradiation time (0–210 minutes) were all examined as photocatalytic degradation variables. The results showed that the $CoFe_2O_4/SiO_2/Ag$ composite was superparamagnetic with a saturation magnetization of 41.82 emu/g and had a band gap of 1.82 eV. The highest efficiency of decreasing the concentration of Congo red dye of 93.70% was obtained with an initial concentration of 10 mg/L, a catalyst dose of 0.5 g/L, and an irradiation time of 180 minutes. This study indicated that the composite had antibacterial properties against Gram-positive (*S. aureus*) and Gram-negative (*E. coli*) bacteria with the same MIC value of 1.25%. These results indicated that the $CoFe_2O_4/SiO_2/Ag$ composite has significant potential for applications in wastewater treatment.

1. Introduction

Environmental pollution by chemicals is a significant problem in the manufacturing process. Therefore, it is necessary to minimize the harmful effects of the waste [1]. In the textile industry, approximately 20–30% of the dye becomes waste during the process [2]. Most dyes are carcinogenic, non-biodegradable, light stable, and ecologically safe [2, 3]. Congo red (CR) is an anionic dye used in the textile industry with diazo and aromatic groups. It is carcinogenic and mutagenic, which causes problems when discharged into the environment [4].

The Advanced Oxidation Process (AOP) is based on the degradation of pollutants using highly reactive species such as hydroxyl radicals (·OH). This method is very suitable for degrading pollutants that are difficult to remove by conventional processes such as coagulation, precipitation, filtration, and more [5, 6, 7]. Among the AOPs, heterogeneous photocatalysis is an attractive method because it has been used to degrade various organic pollutants. This method was conducted at room temperature, which caused total organic mineralization into CO_2, H_2O, and mineral acids [8]. Magnetic ferrite and its composites are promising catalysts with several advantages, such as easy separation from the solution using a permanent magnet after degradation [9].

Among magnetic ferrites, $CoFe_2O_4$ is one compound that has unique properties such as high Curie temperature (Tc~520°C), cubic magneto crystalline anisotropy, and coercivity, as well as a low toxicity, excellent chemical stability, high magnetostrictive coefficient, wear resistance, and moderate magnetization [10, 11, 12]. Several photocatalytic degradation processes have been performed using $CoFe_2O_4$ with a combination of H_2O_2 and visible light for degrading methylene blue dye with an efficiency of 80% [2]. Meso-$CoFe_2O_4/SiO_2$ was also applied to degrade chlorpyrifos with 99.9% [13], while $CoFe_2O_4$-rGO was used for methylene blue, methyl

orange, and rhodamine B dyes with an efficiency of 89%, 64%, and 58%, respectively [14].

Ferrite compounds tend to agglomerate because of their nanoscale sizes. Therefore, it is necessary to modify with other materials to reduce agglomeration. Previous research has shown that non-toxic, environmentally friendly, and biocompatible reagents could be employed to produce materials with superior properties [15]. For instance, Fe_3O_4 is coated with SiO_2 to prevent oxidation, which causes a decrease in magnetic properties, while other reagents increase the stability and compatibility of the composite [16]. Silica (SiO_2) has a hydrophilic surface, which is non-toxic and can promote single-phase formation [17]. Therefore, the coating of $CoFe_2O_4$ using SiO_2 can control particle size and magnetic properties [15, 18].

$CoFe_2O_4$ also shows antibacterial activity that can be applied in the industrial and medical fields [19]. $CoFe_2O_4$ showed antibacterial activity against Gram-negative (*Pseudomonas aeruginosa* and *Escherichia coli*) and Gram-positive (*Staphylococcus aureus* and *Bacillus cereus*) bacteria [20]. The antibacterial activity of $CoFe_2O_4/SiO_2$ can be increased by adding Ag nanoparticles to kill bacteria and antibiotic resistance [21, 22]. Moreover, Ag deposited on the $CoFe_2O_4/SiO_2$ composite improved the antibacterial activity of the nanocomposite and is oxidized to Ag^+ ions, which leads to toxic effects on microorganism cells [23].

In this work, $CoFe_2O_4/SiO_2/Ag$ magnetic composites were synthesized, where $CoFe_2O_4$ was the magnetic core, and SiO_2 and Ag were the inner and outer shells. $CoFe_2O_4/SiO_2$ composite magnetic was used as a photocatalyst to degrade Congo red dye and its ability as an antibacterial agent against *E. coli* and *S. aureus*. These two types of bacteria were selected because they are often available in wastewater.

2. Methodology

2.1. Materials

The reagents were obtained from Merck, including $CoCl_2.6H_2O$, $FeCl_3.6H_2O$, NaCl, HCl, NaOH, NH_4OH, ethanol, Nutrient agar (NA), Dimethylsulfoxide (DMSO), Polyvinylpyrrolidone (PVP), glucose, $AgNO_3$, Tetraethyl orthosilicate (TEOS), and Congo red. The other ingredients used were *Staphylococcus aureus* (ATCC 25923), *Escherichia coli* (ATCC 25922), and distilled water.

2.2. Synthesis of $CoFe_2O_4$

The synthesis of $CoFe_2O_4$ nanoparticles was performed using the coprecipitation method by mixing 3.37 mL HCl (37%) and 2.38 g $CoCl_2.6H_2O$ and dissolving 5.41 g $FeCl_3.6H_2O$ in 20 mL distilled water. The mixture was stirred using a magnetic stirrer for 15 minutes. Subsequently, 2 M NaOH solution was gradually added to the mixture and stirred with a magnetic stirrer at 80℃ until it reached pH 12. The precipitate formed was separated with a permanent magnet and washed several times using distilled water and ethanol until the pH was neutral. The $CoFe_2O_4$ was dried in an oven at 100℃ for 60 minutes and calcined at 400℃ for 2 hours.

2.3. Synthesis of $CoFe_2O_4/SiO_2$ composite

$CoFe_2O_4/SiO_2$ composite was synthesized using the Stöber method with modifications. Approximately 1.5 g of $CoFe_2O_4$ was dissolved in 20 mL of ethanol, and the mixture was stirred using an ultrasonic bath for 20 minutes at room temperature. Subsequently, 5 mL of 6.5 M NH_4OH was added to the mixture and stirred using a magnetic stirrer for 30 minutes. This was followed by adding 10 mL of TEOS and stirring for 4 hours. The product obtained ($CoFe_2O_4/SiO_2$ composite) was washed several times using distilled water and ethanol until the pH was neutral. The $CoFe_2O_4/SiO_2$ composite was dried in an oven at 80℃ for 3 hours.

2.4. Synthesis of $CoFe_2O_4/SiO_2/Ag$ composite

$CoFe_2O_4/SiO_2/Ag$ composite was synthesized using a modified procedure by Nikmah *et al.* [23]. A total of 0.5 g of $CoFe_2O_4/SiO_2$ was dispersed into a 20 mL solution containing 1.27 g PVP, 0.96 g NaOH, and 5.94 g glucose. The mixture was heated and stirred using a magnetic stirrer at 70℃ for 30 minutes. Approximately 5 mL of 0.1 M $AgNO_3$ solution was added dropwise and stirred for 1 hour. The product ($CoFe_2O_4/SiO_2/Ag$ composite) was washed frequently using distilled water and ethanol to obtain a neutral pH. The $CoFe_2O_4/SiO_2/Ag$ composite was dried in an oven at 80℃ for 3 hours.

2.5. Characterization

The structure of the catalyst was identified using an XRD Panalytical with incident radiation Cuα radiation (λ = 1.542 Å) and 2θ range of 10–90°. The average crystal size was calculated using the Scherrer formula. Morphology and elemental catalysts were analyzed by scanning electron microscopy with an energy dispersive spectrometer (SEM-EDS JSM 6510). A vibrating sample magnetometer (VSM Oxford Type 1.2 T) was applied to determine the saturation magnetization value. The absorbance and band gap of the catalyst were identified using UV-Vis Diffuse Reflectance Spectroscopy (Pharmaspec, UV-1700). Congo red dye concentration was determined using a UV-Vis spectrophotometer (Type Orion Aquamate 8000).

2.6. Determination of the pH_{pzc}

The pH_{pzc} was determined using the pH drift method [24]. A total of 25 mL of 0.01 M NaCl solution was adjusted from pH 2 to 11 by adding 0.1 M HCl or 0.1 M NaOH solution. Subsequently, 0.2 g of $CoFe_2O_4/SiO_2/Ag$ composite was added to each Erlenmeyer, and the mixture was stirred using a shaker for 48 hours. The final pH of the solution was measured with a pH meter, and the pH_{pzc} value was determined from a graph plot of ΔpH versus the initial pH.

2.7. Photocatalytic Activity

The photocatalytic activity of the $CoFe_2O_4/SiO_2/Ag$ composite to degrade Congo red dye was determined using a radiation source of 30 W LED lamps (Philips) with a batch reactor. The distance between the light source and the solution was 30 cm. The determined photocatalytic activities include catalyst dose, dye concentration, and irradiation time. The volume of Congo red dye used was

50 mL, the catalyst doses were 0.25, 0.5, 0.75, and 1 g/L, and the dye concentrations were 10, 20, 30, and 40 mg/L. The catalyst was added to the dye solution and stirred using a magnetic stirrer without irradiation for 60 minutes. Subsequently, the irradiation was performed from 0 to 240 minutes, the catalyst was separated from the solution using a magnet, and the concentration of the remaining dye at 30-minute intervals was determined using a UV-Vis spectrophotometer. The dye reduction efficiency was expressed by the ratio of C/C_0, where C_0 and C are the initial and the concentration remaining after photocatalytic degradation.

2.8. Antibacterial test

The antibacterial test was conducted using the Kirby-Bauer disc diffusion method. The concentration of $CoFe_2O_4/SiO_2/Ag$ composite was varied to 0.315%, 0.625%, 1.25%, 2.5%, and 5.0% with DMSO as solvent. The NA medium was poured into a petri dish and mixed with 0.1 mL of each *S. aureus* and *E. coli* solution. Subsequently, the solution was homogenized and allowed to solidify. Paper discs with a diameter of 5 mm were immersed in the composite solution and placed on the surface of the medium using sterile tweezers. The petri dishes were incubated at 37℃ for 24 hours until inhibition zones appeared, while amoxicillin (0.05%) and DMSO were used as positive and negative controls, respectively.

3. Results and Discussion

3.1. Characterization of $CoFe_2O_4$, $CoFe_2O_4/SiO_2$, and $CoFe_2O_4/SiO_2/Ag$ composites

The XRD spectra of $CoFe_2O_4$, $CoFe_2O_4/SiO_2$, and $CoFe_2O_4/SiO_2/Ag$ are shown in Figure 1. The diffraction peaks of $CoFe_2O_4$ were observed at 2θ = 30.53, 35.59, 43.41, 54.15, 57.55, and 63.01, correlated with crystal planes (220), (311), (400), (422), (511), and (440) according to the standard structure of $CoFe_2O_4$ by Joint Committee on Powder Diffraction Standards (JCPDS No. 22-1086) which has spinel cubic type. The $CoFe_2O_4/SiO_2$ composite showed a similar diffraction pattern to $CoFe_2O_4$ but with a lower intensity. This is because the amorphous SiO_2 coating affects the microstructure of the composite [18]. The same pattern on different ferrite compounds, namely Fe_3O_4/SiO_2, decreased in the intensity of Fe_3O_4 spectra after coating with SiO_2 [25].

The XRD spectra of the $CoFe_2O_4/SiO_2/Ag$ composite revealed the presence of additional peaks at 2θ = 38.09, 44.17, 65.45, and 77.11, which is a reflection of the plane (111), (200), (220) and (311) according to JCPDS cards Number 4-0783, showing the structure of Ag in the form of cubic symmetry. The presence of Ag crystal peaks demonstrated that the $CoFe_2O_4/SiO_2/Ag$ composite was successfully synthesized. The crystal size of $CoFe_2O_4$ calculated using the Debye-Scherrer formula obtained a value of 15.4 nm, whereas the crystal size of Ag was 20.6 nm. This value is close to the research of Kalam *et al.* [2], who synthesized $CoFe_2O_4$ using the coprecipitation method ranging from 11.85 to 15.0 nm.

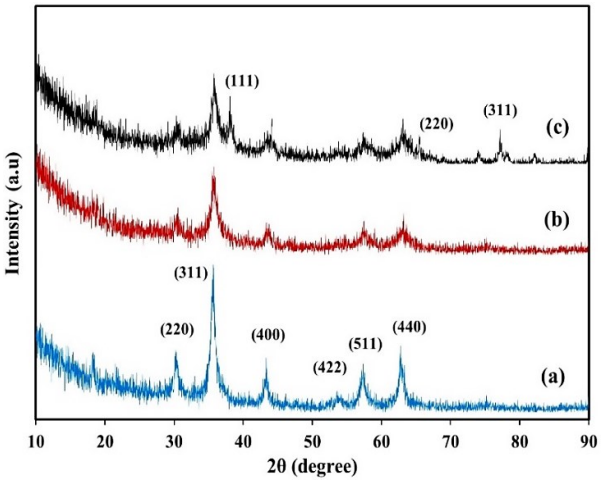

Figure 1. XRD diffraction pattern of (a) $CoFe_2O_4$ (b) $CoFe_2O_4/SiO_2$ (c) $CoFe_2O_4/SiO_2/Ag$ composites

Magnetic properties can be identified from the value of saturation magnetization. Figure 2 shows the magnetic hysteresis loops of $CoFe_2O_4$, $CoFe_2O_4/SiO_2$, and $CoFe_2O_4/SiO_2/Ag$ composites, where the saturation magnetization value of $CoFe_2O_4$ was 54.67 emu/g. The value is lower than bulk $CoFe_2O_4$, which is ± 81 emu/g [26], but it is higher than $CoFe_2O_4$ synthesized using a combustion route, which is 39 emu/g [27]. The magnetic properties of a particle are influenced by particle size and homogeneity [18, 23]. $CoFe_2O_4/SiO_2$ composite sizes 42 and 8 nm had saturation magnetization values of 25 and 10 emu/g, respectively [28]. Therefore, the magnetic saturation values of $CoFe_2O_4/SiO_2$ and $CoFe_2O_4/SiO_2/Ag$ composites were 44.67 emu/g and 41.82 emu/g, respectively. Previous research showed that $CoFe_2O_4$ coating with rGO reduces magnetic dipole interactions between adjacent magnetic particles and isolates the particles from magnetic fields [29].

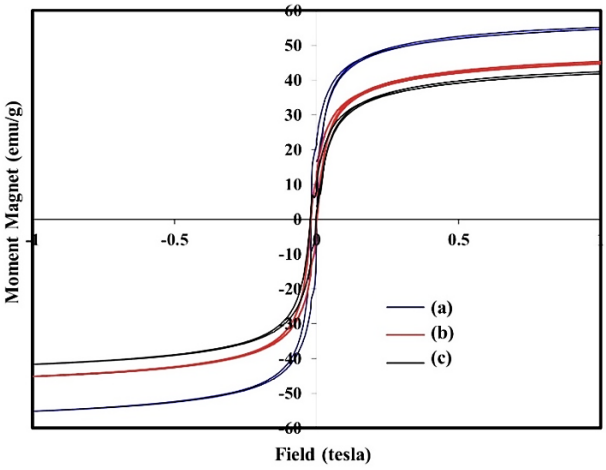

Figure 2. Magnetic hysteresis loops of (a) $CoFe_2O_4$ (b) $CoFe_2O_4/SiO_2$ and (c) $CoFe_2O_4/SiO_2/Ag$ composites

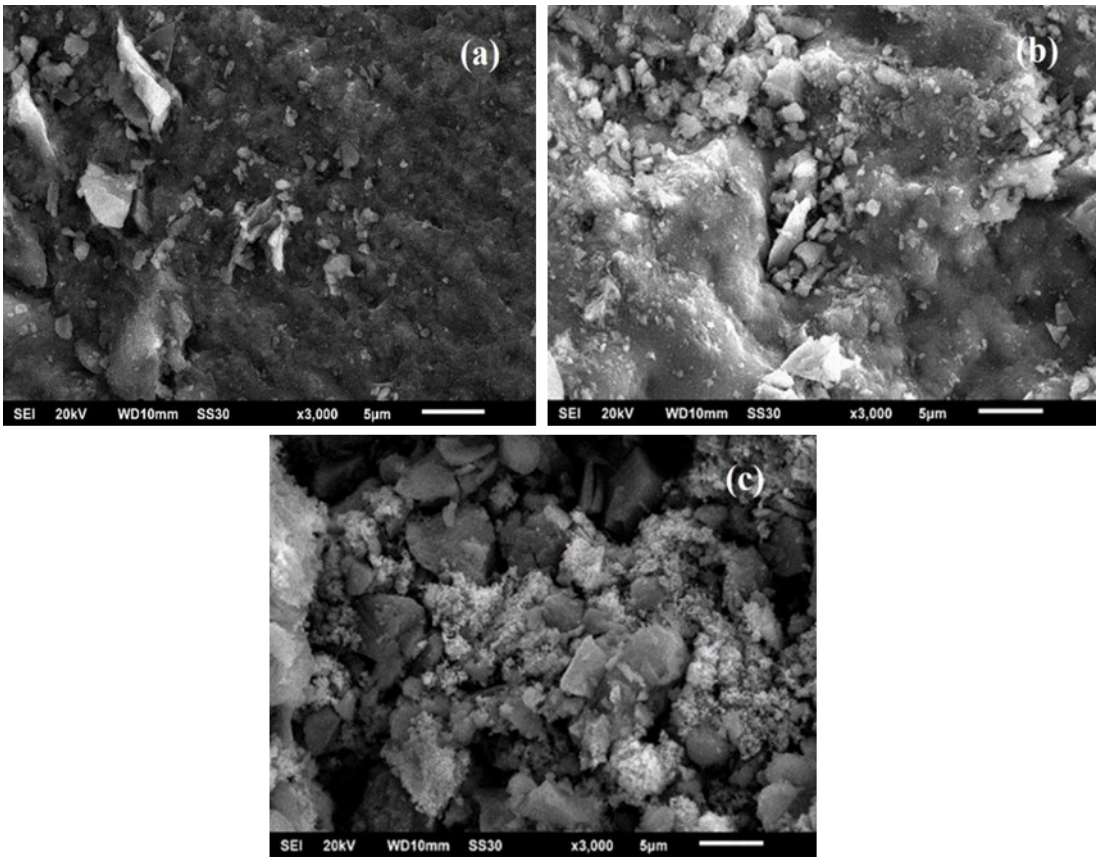

Figure 3. SEM of (a) $CoFe_2O_4$ (b) $CoFe_2O_4/SiO_2$ (c) $CoFe_2O_4/SiO_2/Ag$ composites

The morphology of $CoFe_2O_4$, $CoFe_2O_4/SiO_2$, and $CoFe_2O_4/SiO_2/Ag$ composites with a magnification of 3000× is shown in Figure 3. The surface of $CoFe_2O_4$ is rough and uneven, while the $CoFe_2O_4/SiO_2$ composite appears to have agglomeration due to the coating of SiO_2 on $CoFe_2O_4$. The surface of the $CoFe_2O_4/SiO_2/Ag$ composite was more heterogeneous than $CoFe_2O_4$ and $CoFe_2O_4/SiO_2$ composites. Several small spheres appeared on the surface, indicating that Ag had been dispersed on the surface of the $CoFe_2O_4/SiO_2$ composite.

Figure 4 shows an elemental mapping analysis that indicates the elements in the $CoFe_2O_4/SiO_2/Ag$ composite. The results showed that the $CoFe_2O_4/SiO_2/Ag$ composite was composed of Co, Fe, O, Si, and Ag elements. This confirmed the distribution of elements on the surface of the $CoFe_2O_4/SiO_2/Ag$ composite. Table 1 shows the mass percentages of the constituent elements of $CoFe_2O_4$, $CoFe_2O_4/SiO_2$, and $CoFe_2O_4/SiO_2/Ag$ composites. The presence of Ag in the $CoFe_2O_4/SiO_2/Ag$ composite indicates its dispersion on the surface of the $CoFe_2O_4$-SiO_2 composite.

The amount of light absorbed by the photocatalyst depends on band gap energy, which is the difference between the valence and conduction bands [2]. The UV-DRS spectra and optical band gap energy are shown in Figure 5. The wavelength was observed at 200–750 nm, while the optical band gap determined using the Wood-Tauc equation was obtained at 1.82 eV. The band gap value of $CoFe_2O_4/SiO_2/Ag$ composite < 2.0 eV indicates that $CoFe_2O_4$ dominates the $CoFe_2O_4/SiO_2/Ag$ composite, while $CoFe_2O_4$ has a 1.35 eV. The band gap of pure $CoFe_2O_4$ is ~1.76 eV [30]. Another research showed that $CoFe_2O_4$/rGO and Ag_3PO_4-$CoFe_2O_4$ ~10% had band gaps of 1.75 and 1.4 eV [14, 31].

Table 1. The elemental composition of $CoFe_2O_4$, $CoFe_2O_4/SiO_2$, and $CoFe_2O_4/SiO_2/Ag$ composites

Catalyst	Percentage (%)				
	Co	Fe	O	Si	Ag
$CoFe_2O_4$	24.12	42.59	33.29	-	-
$CoFe_2O_4/SiO_2$	14.11	29.98	46.94	8.97	-
$CoFe_2O_4/SiO_2/Ag$	9.66	18.67	39.38	5.92	26.37

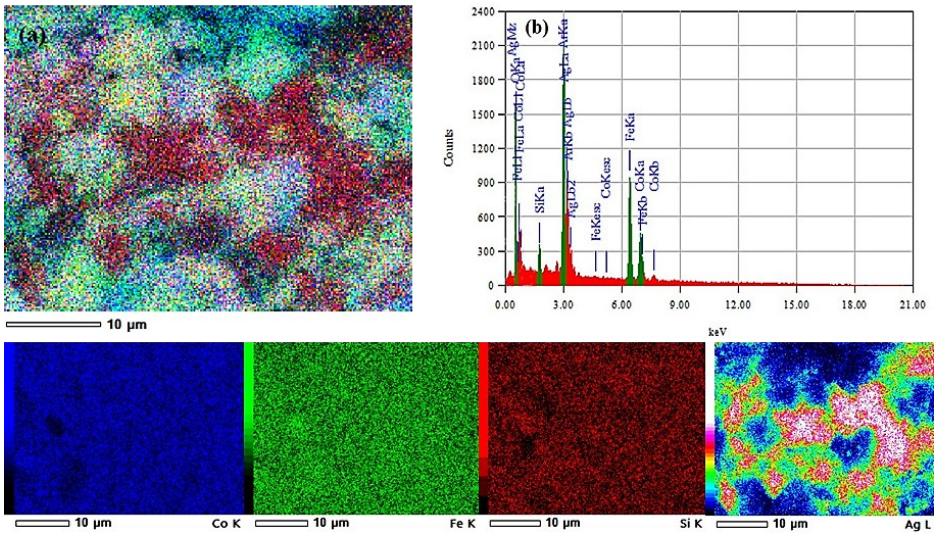

Figure 4. (a) Elemental mapping analysis (b) EDS spectra of $CoFe_2O_4/SiO_2/Ag$ composite

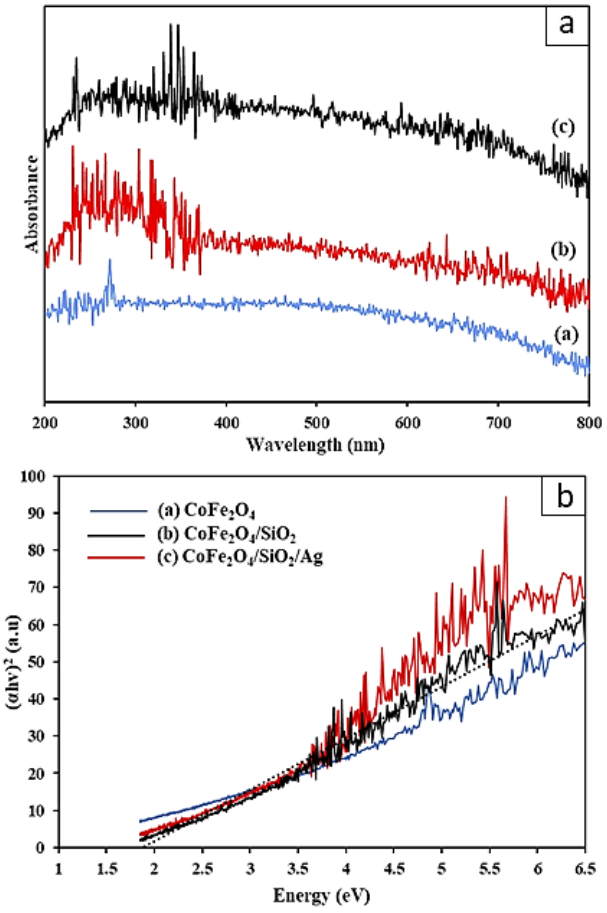

Figure 5. (a) DRS spectra (b) Tauc plot $(\alpha hv)^2$ versus Eg (eV) of $CoFe_2O_4$, $CoFe_2O_4/SiO_2$, and $CoFe_2O_4/SiO_2/Ag$ composites

The pH_{pzc} is the value where the charge on the surface material is zero. Based on Figure 6, the pH_{pzc} of the $CoFe_2O_4/SiO_2/Ag$ composite was obtained at 8.41. The catalyst surface was negatively charged at a solution pH > the pH_{pzc} and positively charged at pH < pH_{pzc} [32]. In this research, pH_{pzc} of $CoFe_2O_4/SiO_2/Ag$ composite was obtained at pH 8.42. The anionic Congo red dye has a high solubility in an acidic pH (pKa = 4.1 at 25°C) and dissociates into $R\text{-}SO_3^-$ [33]. The photocatalytic degradation process is more effective when there is an electrostatic attraction between the negatively and positively charged dye and catalyst. Therefore, the pH of the solution < than pH_{pzc} is effective for the catalytic degradation process. Another research that was carried out using metal selenide-chitosan obtained an optimum degradation at the original pH of the dye in deionized water [34]. At a high pH, the surface of the catalyst becomes more negative due to the presence of OH^- ions, which cause repulsion between the negatively charged dye and the catalyst to reduce the degrading ability [35]. This research used the natural pH of Congo red dye in the range of 5–6.

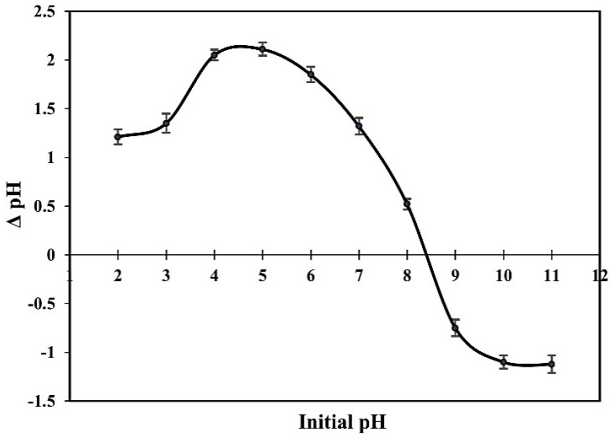

Figure 6. pH_{pzc} of $CoFe_2O_4/SiO_2/Ag$ composite

3.2. Photocatalytic Activity

The photocatalytic degradation of Congo red dye versus irradiation time at various doses of $CoFe_2O_4/SiO_2/Ag$ composite is shown in Figure 7. Congo red dye concentration of 20 mg/L. After the dark adsorption for 60 minutes, it was followed by irradiation. This study indicates that the longer the irradiation, the more Congo red dye will be degraded. The concentration of adsorbed dye increased with a higher dose of $CoFe_2O_4/SiO_2/Ag$ composite (dark adsorption) but not in photocatalytic degradation. The highest reduction in Congo red dye concentrations in the photocatalytic degradation process was at doses of 0.5 and 0.75 g/L, whereas the lowest was at 0.25 g/L. The dye concentration

decreased by 87.2% at a dose of 0.5 g/L. Another research showed that the addition of the catalyst dose did not coincide with the amount of dye degraded, where the photocatalytic degradation of rhodamine B with a volume of 50 mL by $CoFe_2O_4@SiO_2@Dy_2Ce_2O_7$ composite was most excellent at the addition of 4 mg catalyst as compared to 2 and 6 mg [27].

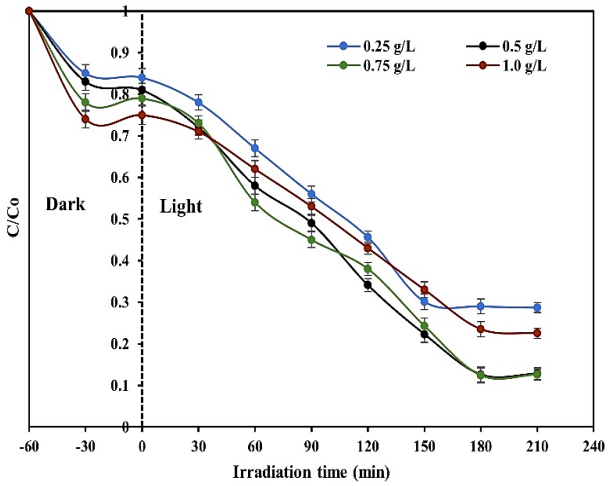

Figure 7. Photocatalytic degradation of Congo red at different catalyst doses

The effect of concentration on the amount of Congo red dye degraded is shown in Figure 8. The dye dose was 0.5 g/L, and the volume was 50 mL with 10, 20, 30, and 40 mg/L concentrations. In this research, the highest degradation efficiency of 93.70% was obtained at a concentration of 10 mg/L. The high concentration of dye blocks causes the catalyst absorbs more light, thereby reducing the photocatalytic degradation performance [36]. In the degradation process, the $CoFe_2O_4/SiO_2/Ag$ composite absorbs energy from light, which leads to the activation of the semiconductor. The photon energy is greater than the photocatalyst band gap energy, and electrons are transmitted from the valence to the conduction band. The electron-hole pair produces oxidative species such as hydroxide and superoxide radicals, which can degrade dyes [30].

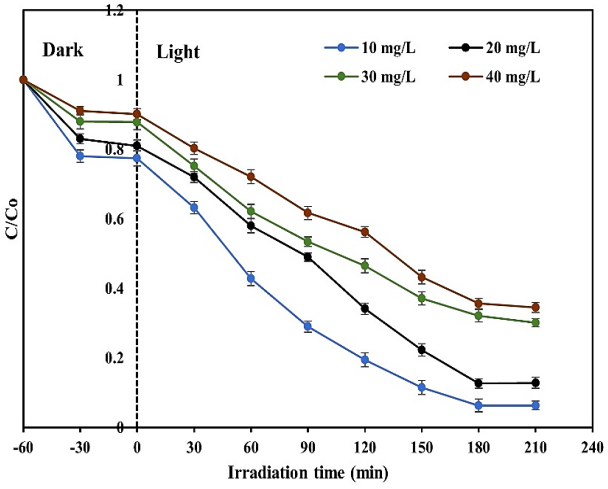

Figure 8. Photocatalytic degradation of Congo red at a different initial dye concentration

Figure 9 shows the performance of $CoFe_2O4$, $CoFe_2O_4/SiO_2$, $CoFe_2O_4/SiO_2/Ag$ composites, and only UV for Congo red dye degradation. The studies employed 10 mg/L of Congo red dye, 0.5 g/L of catalyst, and 180 minutes of irradiation. Photolysis (UV) provides low efficiency (< 5%), indicating the role of the catalyst in the degradation process. $CoFe_2O_4/SiO_2/Ag$ catalyst degradation efficiency is more excellent than $CoFe_2O_4$, $CoFe_2O_4/SiO_2$, and UV. Ag nanoparticles have been widely applied in various catalytic processes. The addition of Ag to $CoFe_2O_4/SiO_2$ increases catalyst performance and stability. The other studies show that $Fe_3O_4/SiO_2/Ag$ catalysts have a greater degradation efficiency than Fe_3O_4/SiO_2 to 4-nitrophenol [37]. SiO_2 serves to protect Fe_3O_4 from agglomeration.

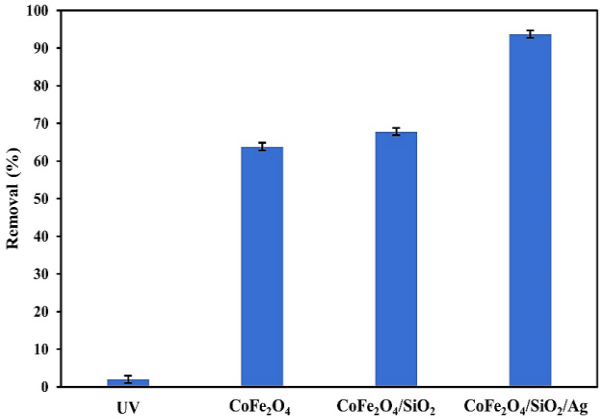

Figure 9. Comparison of photocatalytic degradation of Congo red using UV, $CoFe_2O_4$, $CoFe_2O_4/SiO_2$, and $CoFe_2O_4/SiO_2/Ag$ composites

The mechanism of photocatalytic degradation using $CoFe_2O_4/SiO_2/Ag$ composite is as follows [38, 39]:

$$CoFe_2O_4/SiO_2/Ag + h\nu \rightarrow CoFe_2O_4/SiO_2/Ag\,(e^-_{CB} + h^+_{VB})$$

$$h^+_{VB} + \text{dye} \rightarrow \text{dye}^{\bullet+} \rightarrow \text{oxidation of the dye}$$

Highly reactive species (hydroxyl radicals) result from the breakdown of water molecules or reactions h^+_{VB} with hydroxyl ions.

$$h^+_{VB} + H_2O \rightarrow {}^{\bullet}OH + H^+$$

$$h^+_{VB} + OH^- \rightarrow {}^{\bullet}OH$$

$$^{\bullet}OH + \text{dye} \rightarrow \text{degradation product}$$

The adsorbed oxygen on the catalyst surface reacts with electrons in the conduction band.

$$e^-_{CB} + O_2 \rightarrow {}^{\bullet}O_2^-$$

$$^{\bullet}O_2^- + H_2O \rightarrow HO_2^{\bullet} + OH^-$$

$$^{\bullet}O_2^- + \text{dye} \rightarrow \text{degradation product}$$

$$HO_2^{\bullet} + \text{dye} \rightarrow \text{degradation product}$$

Table 2 shows the photocatalytic degradation of Congo red dye using several catalysts with variable dye concentration, catalyst dose, irradiation time, and dye removal. This study indicates that the $CoFe_2O_4/SiO_2/Ag$ composite can potentially have a better ability in photocatalytic degradation than some current research.

Table 2. Photocatalytic degradation of Congo red dye using several catalysts

Catalyst	Concentration (mg/L)	Catalyst dose (g/L)	Time (h)	Removal (%)	Ref.
Cellulose/PVC/ZnO	50	0.6	2	90	[40]
Mg-TiO_2-P25 NPS	7	0.5	7	80	[41]
$PbTiO_3$	0.0069	0.75	2.5	92	[42]
Bs-$CoFe_2O_4$	5	0.35	1.67	84	[43]
Fs-$CoFe_2O_4$	5	0.35	1.67	87	[43]
As-$CoFe_2O_4$	5	0.35	1.67	92	[43]
$CoFe_2O_4/SiO_2$/Ag	10	0.5	3	93.70	In this study

3.3. Photocatalytic Degradation Kinetics

The kinetics of photocatalytic degradation was determined based on the pseudo-first-order equation as stated below [14, 44]:

$$ln\ C_0/C = kt$$

Where C_0 and C are the concentration of dye before and after photocatalytic degradation (mg/L), k is the apparent rate constant, and t is the irradiation time (minutes). The photocatalytic degradation kinetics at Congo red dye concentrations of 10, 20, 30, and 40 mg/L are shown in Figure 10. The R^2 values close to 1 for all concentrations indicate that the photocatalytic degradation kinetics follows pseudo-first-order. The k value of each concentration was 0.0145, 0.0108, 0.0061, and 0.0055 min^{-1}. There was a decrease in the value of k from the dye concentration of 10 to 40 mg/L. According to Kalam *et al.* [2], the decrease in the rate constant was caused by the fast recombination of electron-hole pairs, which interfered with the photocatalytic degradation process.

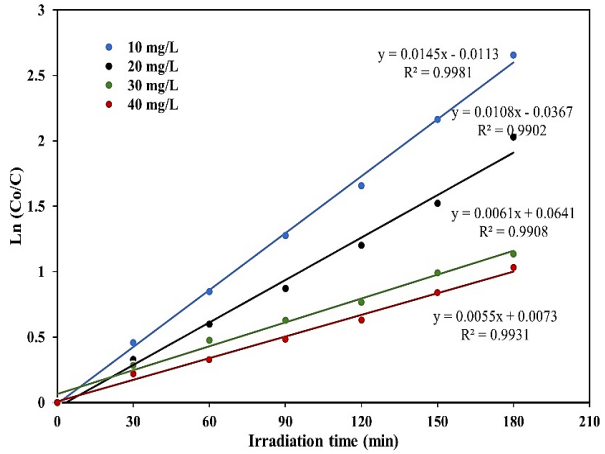

Figure 10. Photocatalytic degradation kinetics of Congo red by $CoFe_2O_4/SiO_2$/Ag composite

3.4. Antibacterial Activity

Table 3 shows the antibacterial properties of $CoFe_2O_4/SiO_2$/Ag composite against *S. aureus* and *E. coli*. The concentration of $CoFe_2O_4/SiO_2$/Ag composite were varied at 0.3125, 0.625, 1.25, 2.5, and 5%. It was discovered that the concentration and size of the material affect the antibacterial properties [45]. The $CoFe_2O_4$ inhibits the growth of *E. coli* and *S. aureus*, where the antibacterial properties against *E. coli* are greater than *S. aureus* [19]. This research obtained the Minimum Inhibitory Concentration (MIC) value at the same concentration of 1.25%; however, the diameter of the inhibition zone of *S. aureus* is smaller than *E. coli* (Figure 11). The presence of SiO_2 on the surface of Fe_3O_4 nanoparticles increases the antibacterial activity by acting as a molecular link between nanoparticles and microorganisms [23].

Table 3. Antibacterial activity of $CoFe_2O_4/SiO_2$/Ag composite

Concentration (%)	Diameter of the inhibition zone (mm)	
	S. aureus	*E. coli*
5	11.10 ± 0.05	11.76 ± 0.08
2.5	9.10 ± 0.09	9.63 ± 0.05
1.25	7.84 ± 0.09	8.43 ± 0.08
0.625	0	0
0.3125	0	0
(+)	19.10 ± 0.12	19.83 ± 0.12
(-)	0	0

The interaction of SiO_2 with cell membranes can change the structure and permeability of bacteria, causing the attraction of metal oxide nanoparticles into the microbial system and damaging the microbial cellular wall [46]. Ag also increases antibacterial activity by damaging bacterial cells through the protein denaturation process. Meanwhile, Ag interacts with functional groups such as protein enzymatic function and accumulates around the microbial cell. The cysteine chain forms –S–Ag bonds, which block the enzymatic function of the protein and inactivate the microbial cell [23, 47].

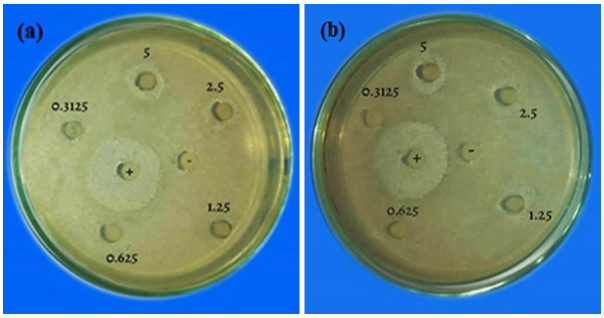

Figure 11. Antibacterial activity of $CoFe_2O_4/SiO_2$/Ag composite against (a) *S. aureus* and (b) *E. coli*

4. Conclusion

Magnetic composites consisting of $CoFe_2O_4$ as core, SiO_2 as shell, and Ag distributed on the surface of SiO_2 were successfully synthesized. The composite was superparamagnetic with a saturation magnetization of 41.82 emu/g and a band gap of 1.82 eV. The efficiency of photocatalytic degradation, with a value of 93.70%, was obtained at a composite dose of 0.5 g/L, 10 mg/L dye concentration, and 180 minutes of irradiation time using UV irradiation. The pseudo-first-order kinetics were suitable to describe the photocatalytic degradation of the Congo red dye with a k value of 0.0145 min^{-1}. $CoFe_2O_4/SiO_2$/Ag composite had antibacterial properties with a MIC value of 1.25% against *S. aureus* and *E. coli*. Therefore, the composite can be developed in wastewater treatment because it has high efficiency in reducing the dye concentration, is easy to separate from the solution using a magnet, and has antibacterial properties.

Acknowledgment

The author thanks the Ministry of Education and Culture, Research and Technology for funding through the Penelitian Dasar Unggulan Perguruan Tinggi (PDUPT) in 2022 with Contract Number 0063.01/UN9.3.1/PL/2022.

References

[1] Talib M. Albayati, Anaam A. Sabri, Dalia B. Abed, Functionalized SBA-15 by amine group for removal of Ni(II) heavy metal ion in the batch adsorption system, *Desalination and Water Treatment*, 174, (2020), 301-310 https://doi.org/10.5004/dwt.2020.24845

[2] Abul Kalam, Abdullah G. Al-Sehemi, Mohammed Assiri, Gaohui Du, Tokeer Ahmad, Irfan Ahmad, M. Pannipara, Modified solvothermal synthesis of cobalt ferrite ($CoFe_2O_4$) magnetic nanoparticles photocatalysts for degradation of methylene blue with H_2O_2/visible light, *Results in Physics*, 8, (2018), 1046-1053 https://doi.org/10.1016/j.rinp.2018.01.045

[3] N. Yahya, F. Aziz, N. A. Jamaludin, M. A. Mutalib, A. F. Ismail, W. N. W. Salleh, J. Jaafar, N. Yusof, N. A. Ludin, A review of integrated photocatalyst adsorbents for wastewater treatment, *Journal of Environmental Chemical Engineering*, 6, 6, (2018), 7411-7425 https://doi.org/10.1016/j.jece.2018.06.051

[4] Youzhou Zhou, Liuqin Ge, Neng Fan, Meisheng Xia, Adsorption of Congo red from aqueous solution onto shrimp shell powder, *Adsorption Science & Technology*, 36, 5-6, (2018), 1310-1330 https://doi.org/10.1177%2F0263617418768945

[5] J. Herney-Ramirez, Miguel A. Vicente, Luis M. Madeira, Heterogeneous photo-Fenton oxidation with pillared clay-based catalysts for wastewater treatment: a review, *Applied Catalysis B: Environmental*, 98, 1-2, (2010), 10-26 https://doi.org/10.1016/j.apcatb.2010.05.004

[6] Andreja Gajović, Adrián M. T. Silva, Ricardo A. Segundo, Saso Šturm, Boštjan Jančar, Miran Čeh, Tailoring the phase composition and morphology of Bi-doped goethite–hematite nanostructures and their catalytic activity in the degradation of an actual pesticide using a photo-Fenton-like process, *Applied Catalysis B: Environmental*, 103, 3-4, (2011), 351-361 https://doi.org/10.1016/j.apcatb.2011.01.042

[7] Luciano Carlos, Debora Fabbri, Alberto L. Capparelli, Alessandra Bianco Prevot, Edmondo Pramauro, Fernando S García Einschlag, Intermediate distributions and primary yields of phenolic products in nitrobenzene degradation by Fenton's reagent, *Chemosphere*, 72, 6, (2008), 952-958 https://doi.org/10.1016/j.chemosphere.2008.03.042

[8] Maria Stylidi, Dimitris I. Kondarides, Xenophon E. Verykios, Pathways of solar light-induced photocatalytic degradation of azo dyes in aqueous TiO_2 suspensions, *Applied Catalysis B: Environmental*, 40, 4, (2003), 271-286 https://doi.org/10.1016/S0926-3373(02)00163-7

[9] Choon Woo Lim, In Su Lee, Magnetically recyclable nanocatalyst systems for the organic reactions, *Nano Today*, 5, 5, (2010), 412-434 https://doi.org/10.1016/j.nantod.2010.08.008

[10] Amit Balsing Rajput, Subhenjit Hazra, Narendra Nath Ghosh, Synthesis and characterisation of pure single-phase $CoFe_2O_4$ nanopowder via a simple aqueous solution-based EDTA-precursor route, *Journal of Experimental Nanoscience*, 8, 4, (2013), 629-639 https://doi.org/10.1080/17458080.2011.582170

[11] Zhigang Jia, Daping Ren, Yongcheng Liang, Rongsun Zhu, A new strategy for the preparation of porous zinc ferrite nanorods with subsequently light-driven photocatalytic activity, *Materials Letters*, 65, 19-20, (2011), 3116-3119 https://doi.org/10.1016/j.matlet.2011.06.101

[12] P. T. Phong, N. X. Phuc, Pham Hong Nam, N. V. Chien, D. D. Dung, P. H. Linh, Size-controlled heating ability of $CoFe_2O_4$ nanoparticles for hyperthermia applications, *Physica B: Condensed Matter*, 531, (2018), 30-34 https://doi.org/10.1016/j.physb.2017.12.010

[13] Huanling Xie, Wenguo Xu, Enhanced activation of persulfate by meso-$CoFe_2O_4/SiO_2$ with ultrasonic treatment for degradation of chlorpyrifos, *ACS Omega*, 4, 17, (2019), 17177-17185 https://doi.org/10.1021/acsomega.9b01626

[14] V. Mahdikhah, S. Saadatkia, S. Sheibani, A. Ataie, Outstanding photocatalytic activity of $CoFe_2O_4$/rGO nanocomposite in degradation of organic dyes, *Optical Materials*, 108, 110193, (2020), 1-13 https://doi.org/10.1016/j.optmat.2020.110193

[15] Thomas Dippong, Erika Andrea Levei, Lucian Diamandescu, Ion Bibicu, Cristian Leostean, Gheorghe Borodi, Lucian Barbu Tudoran, Structural and magnetic properties of $Co_xFe_{3-x}O_4$ versus Co/Fe molar ratio, *Journal of Magnetism and Magnetic Materials*, 394, (2015), 111-116 https://doi.org/10.1016/j.jmmm.2015.06.055

[16] Subramanian Natarajan, Hari C. Bajaj, Rajesh J. Tayade, Recent advances based on the synergetic effect of adsorption for removal of dyes from waste water using photocatalytic process, *Journal of Environmental Sciences*, 65, (2018), 201-222 https://doi.org/10.1016/j.jes.2017.03.011

[17] S. Gowreesan, A. Ruban Kumar, Effects of Mg^{2+} ion substitution on the structural and electric studies of spinel structure of $Co_{1-x}Mg_xFe_2O_4$, *Journal of Materials Science: Materials in Electronics*, 28, 6, (2017), 4553-4564 https://doi.org/10.1007/s10854-016-6091-z

[18] T. Ramesh, S. Bharadwaj, S. Ramana Murthy, $CoFe_2O_4$-SiO_2 Composites: preparation and magnetodielectric properties, *Journal of Materials*, 2016, 7518468, (2016), 1-7 https://doi.org/10.1155/2016/7518468

[19] Noppakun Sanpo, Christopher C. Berndt, Cuie Wen, James Wang, Transition metal-substituted cobalt ferrite nanoparticles for biomedical applications, *Acta Biomaterialia*, 9, 3, (2013), 5830-5837 https://doi.org/10.1016/j.actbio.2012.10.037

[20] Davood Gheidari, Morteza Mehrdad, Saloomeh Maleki, Samanesadat Hosseini, Synthesis and potent antimicrobial activity of $CoFe_2O_4$ nanoparticles under visible light, *Heliyon*, 6, 10, (2020), 1-9 https://doi.org/10.1016/j.heliyon.2020.e05058

[21] Meagan S. Mauter, Yue Wang, Kaetochi C. Okemgbo, Chinedum O. Osuji, Emmanuel P. Giannelis, Menachem Elimelech, Antifouling ultrafiltration membranes via post-fabrication grafting of biocidal nanomaterials, *ACS Applied Materials & Interfaces*, 3, 8, (2011), 2861-2868 https://doi.org/10.1021/am200522v

[22] Monty Liong, Bryan France, Kenneth A. Bradley, Jeffrey I. Zink, Antimicrobial activity of silver nanocrystals encapsulated in mesoporous silica nanoparticles, *Advanced materials*, 21, 17, (2009), 1684-1689 https://doi.org/10.1002/adma.200802646

[23] Ainun Nikmah, Ahmad Taufiq, Arif Hidayat, Sunaryono, Hendra Susanto, Excellent Antimicrobial Activity of $Fe_3O_4/SiO_2/Ag$ Nanocomposites, *NANO: Brief Reports and Reviews*, 16, 05, (2021), 1-13 https://doi.org/10.1142/S1793292021500491

[24] Monika Jain, Mithilesh Yadav, Tomas Kohout, Manu Lahtinen, Vinod Kumar Garg, Mika Sillanpää, Development of iron oxide/activated carbon nanoparticle composite for the removal of Cr(VI), Cu(II) and Cd(II) ions from aqueous solution, *Water Resources and Industry*, 20, (2018), 54-74 https://doi.org/10.1016/j.wri.2018.10.001

[25] Avvaru Praveen Kumar, Dinesh Bilehal, Tegene Desalegn, Shalendra Kumar, Faheem Ahmed, H. C. Murthy, Deepak Kumar, Gaurav Gupta, Dinesh Kumar Chellappan, Sachin Kumar Singh, Studies on synthesis and characterization of $Fe_3O_4@SiO_2@Ru$ hybrid magnetic composites for reusable photocatalytic application, *Adsorption Science & Technology*, 2022, 3970287, (2022), 1-18 https://doi.org/10.1155/2022/3970287

[26] P. C. Rajath Varma, Rudra Sekhar Manna, D. Banerjee, Manoj Raama Varma, K. G. Suresh, A. K. Nigam, Magnetic properties of $CoFe_2O_4$ synthesized by solid state, citrate precursor and polymerized complex methods: A comparative study, *Journal of Alloys and Compounds*, 453, 1-2, (2008), 298-303 https://doi.org/10.1016/j.jallcom.2006.11.058

[27] Sahar Zinatloo-Ajabshir, Masoud Salavati-Niasari, Preparation of magnetically retrievable $CoFe_2O_4@SiO_2@Dy_2Ce_2O_7$ nanocomposites as novel photocatalyst for highly efficient degradation of organic contaminants, *Composites Part B: Engineering*, 174, 106930, (2019), 1-9 https://doi.org/10.1016/j.compositesb.2019.106930

[28] Zbigniew S. Piskuła, Przemysław Skokowski, Tomasz Toliński, Michał Zieliński, Piotr Kirszensztejn, Waldemar Nowicki, Structure, magnetic and catalytic properties of SiO_2-MFe_2O_4 (M= Mn, Co, Ni, Cu) nanocomposites and their syntheses by a modified sol–gel method, *Materials Chemistry and Physics*, 235, 121731, (2019), 1-7 https://doi.org/10.1016/j.matchemphys.2019.121731

[29] Isara Kotutha, Thanawut Duangchuen, Ekaphan Swatsitang, Worawat Meewasana, Jessada Khajonrit, Santi Maensiri, Electrochemical properties of rGO/$CoFe_2O_4$ nanocomposites for energy storage application, *Ionics*, 25, 11, (2019), 5401-5409 https://doi.org/10.1007/s11581-019-03114-1

[30] Sonu, Vishal Dutta, Sheetal Sharma, Pankaj Raizada, Ahmad Hosseini-Bandegharaei, Vinod Kumar Gupta, Pardeep Singh, Review on augmentation in photocatalytic activity of $CoFe_2O_4$ *via* heterojunction formation for photocatalysis of organic pollutants in water, *Journal of Saudi Chemical Society*, 23, 8, (2019), 1119-1136 https://doi.org/10.1016/j.jscs.2019.07.003

[31] Lu Gan, Lijie Xu, Kun Qian, Preparation of core-shell structured $CoFe_2O_4$ incorporated Ag_3PO_4 nanocomposites for photocatalytic degradation of organic dyes, *Materials & Design*, 109, (2016), 354-360 https://doi.org/10.1016/j.matdes.2016.07.043

[32] Anila Ajmal, Imran Majeed, Riffat Naseem Malik, Hicham Idriss, Muhammad Amtiaz Nadeem, Principles and mechanisms of photocatalytic dye degradation on TiO_2 based photocatalysts: a comparative overview, *RSC Advances*, 4, 70, (2014), 37003-37026 https://doi.org/10.1039/C4RA06658H

[33] Ridha Lafi, Imed Montasser, Amor Hafiane, Adsorption of congo red dye from aqueous solutions by prepared activated carbon with oxygen-containing functional groups and its regeneration, *Adsorption Science & Technology*, 37, 1-2, (2019), 160-181 https://doi.org/10.1177%2F0263617418819227

[34] Saraf Khan, Adnan Khan, Nisar Ali, Shehzad Ahmad, Waqar Ahmad, Sumeet Malik, Nauman Ali, Hammad Khan, Sumaira Shah, Muhammad Bilal, Degradation of Congo red dye using ternary metal selenide-chitosan microspheres as robust and reusable catalysts, *Environmental Technology & Innovation*, 22, 101402, (2021), 1-14 https://doi.org/10.1016/j.eti.2021.101402

[35] Subhash Dharmraj Khairnar, Manohar Rajendra Patil, Vinod Shankar Shrivastava, Hydrothermally synthesized nanocrystalline Nb_2O_5 and its visible-light photocatalytic activity for the degradation of congo red and methylene blue, *Iranian Journal of Catalysis*, 8, 2, (2018), 143-150

[36] Poedji Loekitowati Hariani, Muhammad Said, Nabila Aprianti, Yohanna Asina Lasma Rohana Naibaho, High Efficient Photocatalytic Degradation of Methyl Orange Dye in an Aqueous Solution by $CoFe_2O_4$-SiO_2-TiO_2 Magnetic Catalyst, *Journal of Ecological Engineering*, 23, 1, (2021), 118-128 https://doi.org/10.12911/22998993/143908

[37] Yue Chi, Qing Yuan, Yanjuan Li, Liang Zhao, Nan Li, Xiaotian Li, Wenfu Yan, Magnetically separable $Fe_3O_4@$ $SiO_2@TiO_2$-Ag microspheres with well-designed nanostructure and enhanced photocatalytic activity, *Journal of Hazardous Materials*, 262, (2013), 404-411 https://doi.org/10.1016/j.jhazmat.2013.08.077

[38] Muhammad Shahid, Liu Jingling, Zahid Ali, Imran Shakir, Muhammad Farooq Warsi, Riffat Parveen, Muhammad Nadeem, Photocatalytic degradation of methylene blue on magnetically separable $MgFe_2O_4$ under visible light irradiation, *Materials Chemistry and Physics*, 139, 2-3, (2013), 566-571 https://doi.org/10.1016/j.matchemphys.2013.01.058

[39] B. Mercyrani, R. Hernandez-Maya, M. Solís-López, Christeena Th-Th, Photocatalytic degradation of Orange G using TiO_2/Fe_3O_4 nanocomposites, *Journal of Materials Science: Materials in Electronics*, 29, 18, (2018), 15436-15444 https://doi.org/10.1007/s10854-018-9069-1

[40] T. Linda, S. Muthupoongodi, X. Sahaya Shajan, S. Balakumar, Photocatalytic degradation of congo red and crystal violet dyes on cellulose/PVC/ZnO composites under UV light irradiation, *Materials Today: Proceedings*, 2016 https://doi.org/10.1016/j.matpr.2016.04.106

[41] Ujwala O. Bhagwat, Jerry J. Wu, Abdullah M. Asiri, Sambandam Anandan, Sonochemical Synthesis of Mg-TiO_2 nanoparticles for persistent Congo red dye degradation, *Journal of Photochemistry and Photobiology A: Chemistry*, 346, (2017), 559-569 https://doi.org/10.1016/j.jphotochem.2017.06.043

[42] Ujwala O. Bhagwat, Jerry J. Wu, Abdullah M. Asiri, Sambandam Anandan, Photocatalytic degradation of congo red using $PbTiO_3$ nanorods synthesized via a sonochemical approach, *ChemistrySelect*, 3, 42, (2018), 11851-11858 https://doi.org/10.1002/slct.201802303

[43] Nisar Ali, Amir Said, Farman Ali, Fazal Raziq, Zarshad Ali, Muhammad Bilal, Laurence Reinert, Tasleem Begum, Hafiz Iqbal, Photocatalytic degradation of congo red dye from aqueous environment using cobalt ferrite nanostructures: development, characterization, and photocatalytic performance, *Water, Air, & Soil Pollution*, 231, 50, (2020), 1-16 https://doi.org/10.1007/s11270-020-4410-8

[44] Nguyen Thi To Loan, Nguyen Thi Hien Lan, Nguyen Thi Thuy Hang, Nguyen Quang Hai, Duong Thi Tu Anh, Vu Thi Hau, Lam Van Tan, Thuan Van Tran, $CoFe_2O_4$ nanomaterials: Effect of annealing temperature on characterization, magnetic, photocatalytic, and photo-Fenton properties, *Processes*, 7, 12, (2019), 1-14 https://doi.org/10.3390/pr7120885

[45] Poedji Loekitowati Hariani, Fahma Riyanti, Rizki Putri, Salni Salni, Synthesis and characterization of Fe_3O_4 nanoparticles modified with polyethylene glycol as antibacterial material, *The Journal of Pure and Applied Chemistry Research*, 7, 2, (2018), 122-129 http://dx.doi.org/10.21776/ub.jpacr.2018.007.02.393

[46] Azhwar Raghunath, Ekambaram Perumal, Metal oxide nanoparticles as antimicrobial agents: a promise for the future, *International Journal of Antimicrobial Agents*, 49, 2, (2017), 137-152 https://doi.org/10.1016/j.ijantimicag.2016.11.011

[47] Matthew L. Workentine, Joe J. Harrison, Pernilla U. Stenroos, Howard Ceri, Raymond J. Turner, *Pseudomonas fluorescens*' view of the periodic table, *Environmental Microbiology*, 10, 1, (2008), 238-250 https://doi.org/10.1111/j.1462-2920.2007.01448.x